

Kirk Guy J.D. (Orcid ID: 0000-0002-7739-9772)

Boghi Andrea (Orcid ID: 0000-0002-9387-326X)

Soil carbon dioxide venting through rice roots

Guy J.D. Kirk¹ orcid.org/0000-0002-7739-9772 | Andrea Boghi^{1,2} orcid.org/0000-0002-9387-326X | Marie-Cecile Affholder¹ | Samuel D. Keyes² | James Heppell² | Tiina Roose²

¹School of Water, Energy and Environment, Cranfield University, Cranfield MK43 0AL, UK

²Faculty of Engineering and Environment, University of Southampton, Southampton SO17

1BJ, UK

Correspondence

Guy Kirk, School of Water, Energy and Environment, Cranfield University, Cranfield MK43 0AL, UK.

Email: g.kirk@cranfield.ac.uk

Funding information

Biotechnology and Biological Sciences Research Council, Grant Ref. BB/J011584/1

This article has been accepted for publication and undergone full peer review but has not been through the copyediting, typesetting, pagination and proofreading process which may lead to differences between this version and the Version of Record. Please cite this article as doi: 10.1111/pce.13638

Abstract

The growth of rice in submerged soils depends on its ability to form continuous gas channels – aerenchyma – through which oxygen (O_2) diffuses from the shoots to aerate the roots. Less well understood is the extent to which aerenchyma permits venting of respiratory carbon dioxide (CO_2) in the opposite direction. Large, potentially toxic concentrations of dissolved CO_2 develop in submerged rice soils. We show using X-ray computed tomography (CT) and image-based mathematical modelling that CO_2 venting through rice roots is far greater than thought hitherto. We found rates of venting equivalent to a third of the daily CO_2 fixation in photosynthesis. Without this venting through the roots, the concentrations of CO_2 and associated bicarbonate (HCO_3^-) in root cells would have been well above levels known to be toxic to roots. Removal of CO_2 and hence carbonic acid (H_2CO_3) from the soil was sufficient to increase the pH in the rhizosphere close to the roots by 0.7 units, which is sufficient to solubilise or immobilise various nutrients and toxicants. A sensitivity analysis of the model showed such changes are expected for a wide range of plant and soil conditions.

Summary Statement

Large, potentially toxic concentrations of dissolved CO_2 accumulate in submerged paddy soils because CO_2 from plant and soil respiration escapes only very slowly. We found, using X-ray computed tomography and image-based mathematical modelling, venting of soil CO_2 through rice roots at rates equivalent to a third of the daily CO_2 fixation in photosynthesis. Without this venting, the concentrations of CO_2 and associated bicarbonate in root cells would have been well above levels known to be toxic to roots. Removal of soil CO_2 and hence carbonic acid will also affect the solubility and hence plant uptake of various nutrients and toxicants in the rhizosphere.

KEYWORDS

X-ray computed tomography, biological models, biological transport

Acknowledgments

This research was funded by a grant from the UK's Biotechnology and Biological Sciences Research Council (Grant Ref. BB/J011584/1) under the Sustainable Crop Production Research for International Development (SCPRID) programme, a joint multi-national initiative of BBSRC, the UK Government's Department for International Development (DFID) and the Bill & Melinda Gates Foundation.

1 | INTRODUCTION

Large dissolved CO₂ concentrations develop in submerged rice soils (equivalent partial pressures 5–70 kPa – Greenway, Armstrong & Colmer, 2006; Kirk, 2004; Ponnampereuma, 1972) because CO₂ formed in root and soil respiration escapes only slowly by diffusion through the water-filled soil pores. Carbon dioxide is produced in anaerobic respiration in the soil bulk and in aerobic respiration in the rhizosphere fuelled by O₂ and organic substrates released from the roots (Figure 1). There is therefore a large CO₂ gradient between the soil and the aerenchyma inside the root. Hence CO₂ will enter the roots by diffusion and mass flow in the transpiration stream, and be vented to the shoots and atmosphere by diffusion through the aerenchyma (Higuchi, Yoda Tensho, 1984). There has been much research on this pathway for CH₄ emission from ricefields (Butterbach-Bahl, Papen & Rennenberg, 1997; Nouchi, Mariko & Aoki, 1990; Schütz, Seiler & Conrad, 1989; Wang, Akiyama, Yagi & Yan, 2018), but CO₂ – which is > 20 times less volatile than CH₄ – has received little attention. High CO₂ concentrations and associated HCO₃⁻ can be toxic to root cells and therefore some degree of venting is necessary for healthy growth (Greenway et al., 2006). Also removal of dissolved CO₂ will tend to increase the pH of the rhizosphere soil, with consequences for the ricefield biogeochemistry (Affholder, Weiss, Wissuwa, Johnson-Beebout & Kirk, 2017; Begg, Kirk, MacKenzie & Neue, 1994; Kirk & Bajita, 1995). Two further processes affect the chemistry of the rice rhizosphere: oxidation of inorganic reductants, such as ferrous iron, by O₂ from the roots and associated generation of H⁺; and release of H⁺ from the roots to balance excess intake of cations (particularly NH₄⁺) over anions (Kirk, 2004). These inputs of H⁺ will tend to offset H⁺ consumption in venting of dissolved CO₂ from the soil and the resulting changes in carbonate equilibria.

Investigating such processes is challenging given the sensitivity of gas fluxes to measurement conditions. A key problem is how to separate the fluxes of soil-derived CO₂

from those of root- and shoot-derived CO₂. This might be done, for example, with isotopically-labelled carbon sources, if it were possible to ensure uniform labelling and complete separation of the plant and soil sources. In this study we avoided these difficulties by directly imaging and quantifying profiles of gas depletion around rice roots growing in submerged soil using X-ray CT and mathematical modelling.

● In brief, we grew initially 4-week old rice seedlings in a submerged, anaerobic rice soil contained in glass pots, and, after 4 weeks, scanned the pots using X-ray CT imaging to measure the spatial distribution of roots and gas bubbles entrapped in the soil (Figure 1C). The image analysis showed prominent and abundant gas bubbles in the soil bulk, but no or very few bubbles in the soil close to roots, and there was a clear relation between the absence of gas bubbles and high root density, as well as an increasing concentration of bubbles with depth through the soil. Analysis of the bubbles showed they were approximately 40% CO₂ by volume and 60% CH₄. We developed a mathematical model to account for these observations based on the following picture of events.

If the soil solution becomes super-saturated with CO₂ or CH₄, or other volatile products of respiration, gas bubbles will form and tend to become entrapped beneath soil particles. If the bubbles become sufficiently large, or if the soil is agitated by some mechanical disturbance, then the bubbles will rise to the surface by ‘ebullition’. At steady state (which is typically reached within a few weeks of the soil being submerged –Kirk, 2004; Ponnampetuma, 1972), the volume of bubbles and their composition, and the concentrations of dissolved gases in equilibrium with them, will depend on the rates of production versus loss by ebullition and diffusion, and venting through the roots. We fitted the model, based on this outline, to the X-ray CT images of roots and gas bubbles. Thereby we obtained values of the model parameters

and the proportions of CO₂ and CH₄ generated in and leaving the soil via the various pathways. The details follow.

2 | MATERIALS AND METHODS

2.1 | Model development

We describe the steady-state transport of each dissolved gas through the soil by the following continuity equation:

$$\nabla \cdot (D_i \nabla C_{Li} - v C_{Li}) + S_i - E_i - R_i = 0 \quad (1)$$

where C_{Li} is the concentration of dissolved gas i , D_i is its diffusion coefficient through the soil solution, v is the water flux into roots, S_i is the rate of gas production, E_i is the rate of ebullition and R_i is the rate of root-mediated efflux. There is an equation of this form each for dissolved CO₂, CH₄ and N₂, which enters the soil by diffusion from the atmosphere and roots. For CO₂, C_{Li} is adjusted for the concentration of dissolved CO₂ plus the concentration of HCO₃⁻ in equilibrium with it (CO₃²⁻ is unimportant at the near neutral pH of most submerged soils).

In Equation 1, the diffusion coefficient, $D_i = D_{Li} \theta_L f_L$ where D_{Li} is the diffusion coefficient in free solution, θ_L is the soil volumetric water content, and f_L is a tortuosity factor (Kirk, 2004). The volumetric gas content, θ_G (from which $\theta_L = \theta - \theta_G$ where θ is the total porosity) is proportional to the sum of the partial pressures of the volatile solutes,

$\sum P_i = P_{CO_2} + P_{CH_4} + P_{N_2} + P_{H_2O}$ (P_{H_2O} is the saturating pressure of H₂O):

$$\theta_G = K_\theta \sum P_i \quad (2)$$

where K_θ is a constant that is characteristic of the submerged, puddled soil. From the gas law:

$P_i = RT C_{Gi}$ where C_{Gi} is the concentration of gas i in the soil gases. From Henry's law:

$C_{Gi} = C_{Li} / K_{Hi}$ where K_{Hi} is the dimensionless Henry's law constant for gas i .

We specify the following relations for S_i , E_i and R_i . For S_i , at steady-state, CO_2 production from soil carbon is constant with depth and time, equal to $S_{\text{CO}_2,0}$, and production from root-derived carbon is proportional to the root length density, L_V (root length per unit soil volume), i.e.

$$S_{\text{CO}_2} = S_{\text{CO}_2,0} + k_V L_V \quad (3)$$

where k_V is a proportionality constant. At steady state, the ratio of CH_4 production to CO_2 production is also constant (Kirk, 2004):

$$S_{\text{CH}_4} = \alpha_{\text{CH}_4} S_{\text{CO}_2} \quad (4)$$

For E_i , the rate of ebullition is a function of the volume of the gas bubbles: as bubbles grow, they become more buoyant and so are more easily displaced. Hence, taking total gas volume to represent bubble volume:

$$E_i = k_E \theta_G C_{Gi} \quad (5)$$

where k_E is a rate constant which depends on the physical properties of the soil. For R_i , root-mediated efflux from the soil occurs by degassing of dissolved CO_2 and CH_4 into the root aerenchyma and diffusion through the aerenchyma to the atmosphere (Beckett, Armstrong, Justin & Armstrong, 1988). We represent this as:

$$R_i = k_T L_V D_{Gi} (C_{Gi} - C_{Gi0}) \quad (6)$$

where k_T is a root gas transmissivity, D_{Gi} is the diffusion coefficient of gas i in air, C_{Gi} is the gas concentration along the profile and C_{Gi0} is the gas concentration at $z = 0$. The root gas transmissivity accounts for all factors limiting CO_2 transfer from the soil solution at the root surface to the aerenchyma at the base of the roots at $z = 0$, including the gas permeability of the root wall and epidermis, and the root porosity.

We solved Equations 1–6 subject to C_{Li} being constant at the soil-floodwater boundary and there being no flux of gases across the lower boundary. We fitted the model to the observed profiles of gas content by optimizing the values of k_v , k_E and k_T ; all the other parameters were derived independently, and a single set of values was fitted for all replicates and both planting densities (Section 2.4 and Table 1).

2.2 | Experimental methods

We used the same soil, rice genotype and growth conditions as Affholder et al. (2017). In brief, 4-week old rice seedlings, grown in nutrient culture, were transplanted into pots of submerged, anaerobic rice soil at either 1 or 4 plants per pot planted closely together. After 4 weeks the pots then scanned using X-ray CT imaging to measure the spatial distribution of roots and gas bubbles entrapped in the soil (Section 2.3).

The soil was from rice fields at Tiaong, Quezon Province, Philippines. It is a Hydraquent (USDA Soil Taxonomy). Portions of topsoil (0–30 cm depth) were air dried and sieved to pass < 2 mm. The properties of the sieved soil were 42% clay, 40% silt, pH (aerobic in H_2O) 8.5, CEC 9.0 $cmol_c\ kg^{-1}$, organic carbon content 73 $g\ kg^{-1}$ and carbonate content 96 $g\ kg^{-1}$ (Izquierdo, Impa, Johnson-Beebout, Weiss & Kirk, 2016).

Portions (1.2 kg) of the air dried soil were mixed with 10 $g\ kg^{-1}$ of rice straw, to stimulate anaerobic reduction processes, and then saturated with deionized water and puddled to make a slurry. The slurry was poured into 10-cm internal diameter, 21-cm deep, cylindrical, thin-walled (3-mm) Perspex pots to a depth of 17 cm. The resulting soil bulk density was 0.81 $kg\ dm^{-3}$ and the volumetric water content was 0.69. The filled pots were inserted into 12-cm diameter, 21-cm deep glass pots, and the space between the inner and outer pots filled with further slurry. This arrangement ensured anoxic conditions in the soil in the inner pot, while the thin Perspex wall of the pot was completely transparent to X-rays for imaging after removal from the outer pot. Further deionized water was added to bring the level to the top of

the pots, and the water standing in the pots was maintained at this level through the experiment. The soil was allowed to become reduced for 4 weeks at 30°C before transplanting the rice seedlings.

Rice seeds (CV IR55179) were germinated in petri dishes at 30°C in complete darkness for 3 days. The germinated seeds were transferred to a mesh floating on Zn-free Yoshida nutrient solution (Yoshida, Forno, Cook & Gomez, 1976), and grown for 4 weeks before being transplanted manually into the pre-reduced soil in pots. The seedlings were placed with the root crown at approximately 5 cm below the soil-floodwater boundary, as is the practice for growing rice in this soil in the field because of its loose structure and hence weak support for seedlings (Mori et al., 2016). The growth conditions – both before and after transplanting – were 13.5 h light ($600 \mu\text{mol m}^{-2} \text{s}^{-1}$ white light) at 30°C and 10.5 h dark at 24°C.

At 4 weeks after transplanting, the inner Perspex pots were removed and the roots and soil in the pots were imaged as described below. The imaging was complete within 24 h. The aerial plant parts were then separated from roots at the root crown limit. The fresh biomass was measured, and tillers and leaf number counted. They were then thoroughly washed with UHP water and dried at 70°C for 5 days.

Further pots were set up in the same way, but left unplanted to measure gas productions in the bulk soil following flooding. Each pot was fitted with a rhizon solution sampler (Rhizosphere research products, Wageningen, Netherlands) with a 5-cm porous section, and fitted with a Luer lock. The samplers were held vertically in the soil so that the porous section ran from 8.5 to 13.5 cm below the floodwater-soil boundary. At weekly intervals, solution was withdrawn and analysed for dissolved CO_2 (MI-720 electrode, Microelectrodes Inc, USA) and pH (MI-410 combination electrode, Microelectrodes Inc, USA). Redox potential was monitored with a Pt electrode. The composition of gas bubbles accumulated in the soil was monitored by periodically fitting over each pot a 3 dm³ gas-tight bag fitted with a

sampling port, and agitating the pots to displace entrapped soil gases into the headspace.

Samples of the headspace were withdrawn by syringe and analysed for CO₂ and CH₄ by gas chromatography (Cambridge Scientific Instruments 200 Series GC).

We estimate the pH buffer power (i.e. the amount of base required to produce unit increase in pH; b_{HS}) of the submerged, reduced soil from the results of Affholder et al. (2017) who found with the same rice genotype and growth conditions as here that the pH averaged over the root zone increased by 0.34 pH units due to a net removal of H⁺ as H₂CO₂ through the roots of 11.0 mmol kg⁻¹, but offset by a net addition of 1.6 mmol H⁺ kg⁻¹ from the roots to balance excess intake of cations over anions. On the basis of the soil Fe(II) concentration, the addition of H⁺ in Fe(II) oxidation by the roots was far smaller. Hence $b_{HS} = (11.0 - 1.6)/0.32 = 29 \text{ mmol kg}^{-1} \text{ pH}^{-1}$.

2.3 | X-ray CT Imaging

Roots and gas bubbles in the pots were imaged using a Custom Nikon/XTEK Hutch X-ray CT scanner. The field of view was 8 cm in diameter and 5.6 cm in height, with the upper edge approximately at the base of the primary roots, 5-cm below the soil-floodwater boundary. The pots were scanned at 120 kV and 185 uA. A 1 mm copper filter was used to minimise beam hardening. A total of 3001 angular projections through 360° were acquired at an exposure of 177 ms, with 32-frame averaging for each projection. The scan duration was 4.7 h per sample, and the resulting voxel size was 40 µm (isotropic). Data were reconstructed using a filtered back-projection algorithm implemented in Nikon CTPro 3D, generating 32-bit volumes which were subsampled to produce a stack of two-dimensional 8-bit TIFF files for each scan. A modest beam hardening correction was applied during reconstruction.

Gas bubbles were extracted from the data by 3D median filtering using an 8 × 8 × 8 voxel cubic kernel, then hysteresis thresholding, using the Fiji image-analysis software (Schindelin et al., 2012). Aerenchymatous roots were extracted using a region-growth method (Keyes et

al., 2013) followed by manual analysis of remaining roots in Avizo 9.0.0. The gas bubble geometry was subtracted from the root geometry to remove co-classified voxels. The spatial distributions of roots and gas were classified with respect to pot depth and radial distance from a vertical axis through the centre of the plants using code written in MATLAB 2018b (MathWorks, Massachusetts, USA).

We transformed the scanned root and gas data into volumetric spatial data (root length density, L_V , and volumetric gas content, θ_G) using the conversion that one voxel edge length was equivalent to 0.04 mm. Each scan was 5.8 cm (1450 pixels) in depth, with approximately 5 cm of soil above the upper edge and 6 cm below the lower edge. The L_V and θ_G data were extrapolated over the entire depth by fitting three-dimensional Gaussian distributions to the pooled data for the three replicates for each planting density:

$$X(r, z) = A \exp \left[-\frac{\{(r - r_0) \cos \varphi + (z - z_0) \sin \varphi\}^2}{2\sigma_r^2} - \frac{\{(r - r_0) \sin \varphi + (z - z_0) \cos \varphi\}^2}{2\sigma_z^2} \right] \quad (7)$$

where X is either L_V or θ_G and φ , σ_r and σ_z are the corresponding fitting coefficients.

Parameters were fitted in MATLAB using the *fmincon* function to minimize the square difference between the measurements and Equation 7.

2.4 | Model parameterisation

We solved Equation 1 for each of the three gases CO_2 , CH_4 and N_2 subject to the stated boundary conditions and Equations 2–6 using standard numerical methods. We parameterised the model as follows.

Firstly we used pre-set values of the following parameters: (a) the three-dimensional distribution of L_V obtained from the root images as described in the previous section; (b) K_θ , $S_{\text{CO}_2,0}$ and α_{CH_4} in Equations 2–4 by running the model with no roots (i.e. no rhizo-deposition and no gas venting through the roots) to fit the observed concentration of dissolved CO_2 and

pH in the unplanted bulk soil and the ratio of CO₂ to CH₄ measured in entrapped gases displaced from the soil; and (c) all other variables, except k_E , k_T and k_V , based on the experimental data and standard values for the constants and coefficients (Tables 1 and S1, Supporting information).

We then fitted values of k_E , k_T and k_V by running the model to obtain the best agreement between our observed and predicted three-dimensional profiles of θ_G for each planting density, using the MATLAB *fmincon* function. A unique set of k_E , k_T and k_V values was found for the whole dataset by minimizing the average of the fitting errors calculated for the individual replicate runs.

The rate of generation of CO₂ in the soil per unit soil surface was calculated from

$$J_S = S_{CO_2,0}L + k_V \frac{2}{R^2} \int_0^L \int_0^R L_V \cdot r dr dz \quad (8)$$

where L and R are the depth and radius of the soil volume, respectively. The flux through the roots was calculated from

$$J_R = k_T D_{G,CO_2} \frac{2}{R^2} \int_0^L \int_0^R L_V (C_{G,CO_2} - C_{G,CO_2,0}) \cdot r dr dz \quad (9)$$

The flux from the soil surface by ebullition was calculated from

$$J_E = k_E \frac{2}{R^2} \int_0^L \int_0^R \theta_G C_{G,CO_2} \cdot r dr dz \quad (10)$$

The flux from the soil surface by diffusion was calculated from

$$J_D = J_S - J_R - J_E \quad (11)$$

Copies of the experimental data and the source code for the model written in FORTRAN are available from <https://doi.org/...>

3 | RESULTS

3.1 | Model fits

Figure 2 and Figures S1 and S2 in the Supporting Information give the measured and modelled results for 4 plants per pot, and Figures S3–S5 in the Supporting Information give the results for 1 plant per pot. Figure 3 gives the calculated profiles of the different gases through the soil from the model runs in Figure 2. The fitted k_V , k_E and k_T values (Table 1) are realistic (Section 3.2). So, given experimental errors, the good agreement between the observed and predicted results for both planting densities and all replicates suggests all the important processes have been satisfactorily allowed for.

3.2 | Sensitivity analysis

Figure 4 shows the sensitivity of the model to its input parameters. For the standard parameter values, the rate of CO₂ production from soil carbon per pot ($= S_{\text{CO}_2,0} \times \text{soil volume}$) = 0.016 mol d⁻¹, and the flux of CO₂ through the roots per pot ($= J_R \times \text{soil surface area}$) = 0.005 mol d⁻¹. The plant shoot growth over 28 d was 2.2 ± 0.4 g dry weight per pot ≈ 0.073 mol C. Assuming exponential growth and equal root and shoot growth, this is equivalent to approximately 0.015 mol d⁻¹ after 28 d. So the CO₂ flux through the roots was approximately a third of the daily rate of photosynthesis. For the standard values, the proportions of total CO₂ escaping through the roots and by diffusion and ebullition from the soil surface are 28, 14 and 58%, respectively, and the proportions of CH₄ escaping via these pathways are 18, 1 and 81%, respectively.

Over the 100-fold range in values shown in Figure 4, the fluxes through all three routes are most sensitive to the soil-carbon derived respiration, $S_{\text{CO}_2,0}$. The fluxes are also sensitive to the ebullition rate constant, k_E , and the constant K_θ in Equation 2. However these are fitting parameters for the soil, and are themselves sensitive to the value of $S_{\text{CO}_2,0}$, a large E_i

following from a large S_i in Equation 1; so they are less relevant to our main theme of venting through the roots. The constant for root-carbon derived respiration, k_v , is unimportant at the high $S_{\text{CO}_2,0}$ value of our humose experimental soil; it will be more important at lower $S_{\text{CO}_2,0}$ values. The CO_2 and CH_4 fluxes are also sensitive to the ratio of CH_4 to CO_2 production, α_{CH_4} and the root gas transmissivity, k_T .

4 | DISCUSSION

4.1 | Parameter values

Wide ranges in $S_{\text{CO}_2,0}$ and k_v values are expected. The rice field carbon economy – and hence $S_{\text{CO}_2,0}$ – depends on the soil's initial organic matter content and on management of crop residues and organic manures (Greenland, 1997). Common practice is to remove part of the straw during the harvest and to burn the straw produced after threshing (Fairhurst, Witt, Buresh & Dobermann, 2007; Greenland, 1997). The stubbles and roots are incorporated into the soil during land preparation for the following crop, and they decompose over the course of the crop. Inputs of carbon from roots – and hence k_v – are as soluble exudates, insoluble secretions and detrital root material, and are also highly variable. They depend on growth conditions, healthy plants tending to be less leaky (Rose et al., 2013; van der Gon et al., 2002); and on genotype, modern rice varieties bred for high grain yield having leaner and less leaky roots than traditional varieties (Jiang et al., 2013; Maurer, Kiese, Kreuzwieser & Rennenberg, 2018; van der Gon et al., 2002).

The ratio of CH_4 to CO_2 production, α_{CH_4} , depends on (a) the presence of inorganic oxidants, and (b) the stoichiometry of methanogenic soil organic matter decomposition and the resulting proportions of CH_4 produced from disproportionation of acetate versus reduction of CO_2 with H_2 (Reactions 2–4, Figure 1) (Yao & Conrad, 2000). In general the former

dominates (Yao & Conrad, 2000), and $\alpha_{\text{CH}_4} = 1$ is typical (Kirk, 2004). A large proportion of the CH_4 flux will be oxidized to CO_2 by methanotrophic bacteria in the rhizosphere and oxic floodwater-soil interface; up to 95% of the root-mediated CH_4 flux is oxidized to CO_2 (Arah & Kirk, 2000; Cho, Schroth & Zeyer, 2012; Hernández, Dumont, Yuan & Conrad, 2015; Reid, Pal & Jaffe, 2015; van Bodegum, Stams, Mollema, Boeje & Leffelaar, 2001). The net root CO_2 flux will be correspondingly greater.

The root gas transmissivity, k_T , depends on such variables as aerenchyma volume fraction, the permeability of root tips and laterals, root architecture and growth stage (Kirk, 2003; Yamauchi, Colmer, Pederson & Nakazono, 2018). The value of k_T will also influence the degree of aerobic CO_2 generation and CH_4 oxidation in the rhizosphere. Other things being equal, a high k_T value reduces rather than enhances net CH_4 emission because it allows increased oxygenation of the rhizosphere (Arah & Kirk, 2000; Jiang et al., 2017). There isn't much published information with which to judge our k_T values directly. However from the wealth of information on the root pathway for CH_4 emissions from rice, our root fluxes of CO_2 are highly plausible.

4.2 | Mechanisms of CO_2 entry into the root

To reach the aerenchyma in the root cortex, dissolved CO_2 and HCO_3^- in the soil solution must pass through the root wall and epidermal tissues. Under anoxic conditions in submerged soil, the rice root system develops a layer of suberized cells in the walls of primary roots starting 1–1.5 cm behind the root tip (Yamauchi et al., 2018). This layer is highly impermeable to O_2 – and by implication to CO_2 – and so restricts radial loss of O_2 to the soil and thereby allows a greater length of root to be aerated (Yamauchi et al., 2018). The rice root system typically comprises coarse, aerenchymatous, primary roots with gas-impermeable walls conducting O_2 to short, fine, gas-permeable laterals, which have a much

greater surface area per unit mass than the primary roots. Kirk (2003) shows that this architecture provides the greatest absorbing surface for nutrients per unit aerated root mass. The same argument would apply to the absorption of CO_2 by the root system. A further pathway for soil CO_2 into the aerenchyma may be via the basal stem tissue at the root-shoot junction below the soil surface (Pedersen, Pulido, Rich & Colmer, 2011).

After crossing the root wall, the dissolved CO_2 in the root apoplast must pass through the epidermal tissue. The passive apoplastic route through the epidermis is obstructed by the Casparian strip, and so CO_2 or HCO_3^- or both must cross the plasma membrane into the symplasm. While uncharged CO_2 molecules can pass through cell walls passively, HCO_3^- anions cannot. This is problematic because there are no known membrane transporters for HCO_3^- in higher land plants (Bloemen, McGuire, Aubrey, Teskey & Steppe, 2013; Poschenrieder et al., 2018; Shimono, Kondo & Evans, 2019). A boron transporter, BOR1, is reported to be homologous to an animal HCO_3^- transporter (Takano et al., 2002), but there is as yet no evidence that it functions as such in plants. This implies HCO_3^- must be converted into CO_2 , which then diffuses to the cortex via the symplasm.

At the pH of the soil bulk in our experiment (7.0), 82% of the dissolved CO_2 (H_2CO_3^* plus HCO_3^-) is in the form of HCO_3^- . Removal of CO_2 from the soil close to root surfaces will tend to raise the soil pH (Section 4.5). But the root apoplast is generally acidified to some extent: Felle (2001) gives values below pH 6. At pH 6.5, the proportions of dissolved CO_2 and HCO_3^- are nearly equal, so the apoplastic-symplastic route will be greatly enhanced to the extent that the apoplast is acidified. We know of no studies of root apoplastic pH in rice. But given that, in general, the main form of N taken up in paddy soils is NH_4^+ , so that cation uptake exceeds anion uptake, the apoplast is likely to be acidified. Geilfus (2017) reviews methods for measuring apoplastic pH.

The uncatalysed CO_2 hydration-dehydration reactions, by which H_2CO_3 and hence HCO_3^- equilibrates with CO_2 ($\text{HCO}_3^- + \text{H}^+ = \text{H}_2\text{CO}_3 = \text{CO}_2 + \text{H}_2\text{O}$), are slow, and so may be rate-limiting for the apolastic-symplastic pathway or degassing of CO_2 into the aerenchyma or both. The presence of carbonic anhydrase, which catalyses the reactions, in the apoplast is therefore an important question. Cytosolic carbonic anhydrase is ubiquitous in plant tissues (DiMario, Clayton, Mukherjee, Ludwig & Moroney, 2017) but its presence in the apoplast is less certain (Savchenko, Wiese, Neimanis, Hedrich & Heber, 2000).

4.3 | Fate of the CO_2 in the root

Is the concentration of CO_2 and associated HCO_3^- in the roots sufficient to be toxic? The soil CO_2 concentration in our experiment was equivalent to $P_{\text{CO}_2} \approx 20$ kPa in the soil bulk but 10-fold less than this at the root surface as a result of venting through the roots. Plant species well adapted to high P_{CO_2} in the root zone, such as rice, can thrive at P_{CO_2} values well above 20 kPa through mechanisms that are not well understood (Greenway et al., 2006). If the cytoplasm was in equilibrium with $P_{\text{CO}_2} = 20$ kPa, and the pH was maintained at the typical value of 7.5 through the biochemical and biophysical pH stats, then the cytoplasmic HCO_3^- concentration would be approximately 90 mM, which is above values at which metabolism is impaired (of the order of 50 mM or possibly as low as 10 mM for some enzyme systems – Greenway et al., 2006). Whereas at $P_{\text{CO}_2} = 2$ kPa, as calculated for the soil at the root surface, the HCO_3^- concentration would be only about 9 mM, which is in the normal range (2–20 mM) and well-below toxic levels. This indicates the rate of CO_2 venting through the roots would be sufficient to avoid toxic concentrations in root cells.

In fact, the enhanced availability of CO_2 in the roots may have a growth stimulating effect in rice by facilitating anaplerotic production of organic acids for amino acid synthesis (Balkos, Britto & Kronzucker, 2010; Britto & Kronzucker, 2005). In general, the main form

of N taken up by rice in submerged soils is NH_4^+ , and virtually all the NH_4^+ is assimilated into amino acids in the roots before being transported to the shoots (Kronzucker, Siddiqi, Glass & Kirk, 1999). This occurs via glutamine synthetase (GS), which catalyses the incorporation of NH_4^+ into the organic pool, and phosphoenolpyruvate carboxylase (PEPC) which fixes CO_2 into oxaloacetate and malate so providing carbon skeletons for the GS pathway. In principle, if other factors are non-limiting, increased CO_2 supply in the roots would allow greater N assimilation.

The PEPC pathway might be a significant sink for root CO_2 . An upper estimate of the size of this sink can be got from the rate of N uptake by the roots with the crude assumption that all the N is taken up as NH_4^+ and assimilated via GS and PEPC. From the plant growth rate (0.45 g d^{-1} at 28 d after transplanting – Section 3.2) and N content (approximately 15 mg g^{-1} – Affholder et al., 2017), the rate of N uptake was approximately 0.48 mmol d^{-1} , which is less than 10% of the CO_2 flux through the roots. In fact, a significant part of N uptake by rice in submerged soils is as NO_3^- , formed by nitrification of NH_4^+ in the rhizosphere (Kirk & Kronzucker, 2005), and most of the NO_3^- will be assimilated in the shoots rather than the roots (Kronzucker et al, 1999). We conclude the flux of CO_2 through PEPC in the roots will be small compared with the net CO_2 flux. This is consistent with the assumption implicit in the model that at steady state, effectively all the CO_2 entering the roots diffuses to the shoots via the aerenchyma (Equation 6).

4.4 | Fate of the CO_2 reaching the shoot

Could recycling of root- and soil-derived CO_2 through the roots to the shoots provide a source of CO_2 for photosynthesis? The soil-derived CO_2 flux through the plants was equivalent to approximately a third of the daily rate of photosynthesis, i.e. 20% of the actual rate of photosynthesis given that the photo-period was 13.5 h. This suggests a large potential source for photosynthesis. We know of no data on this point for rice plants. However

measurements with emergent wetland plants such as *Phragmites* suggest sediment-derived CO_2 accounts for less than 1% of the carbon fixed by the shoots (Brix, 1990; Constable & Longstreth, 1994; Singer, Eshel, Agami & Beer, 1994). Although aerenchyma provides a continuous gas pathway between the roots and leaves, the stems of rice plants contain lenticels which allow gas exchange with the atmosphere in the lower part of the canopy (Yamauchi et al., 2018). So the bulk of the root-borne CO_2 probably escapes from the aerenchyma before reaching the main photosynthetic tissue.

4.5 | Other implications

Removal of soil CO_2 through the roots has important implications for the chemistry of the rhizosphere. Removal of dissolved CO_2 and hence H_2CO_3 will tend to increase the rhizosphere pH. The maximum depletion of $\text{H}_2\text{CO}_3 + \text{HCO}_3^-$ by the roots (Figure 3) was 30 mM, i.e. 21 mmol kg^{-1} , allowing for the soil water content and bulk density. Hence, from the pH buffer power of the soil ($b_{\text{HS}} = 29 \text{ mmol kg}^{-1} \text{ pH}^{-1}$, Section 2.2) the expected pH increase close to the roots is 0.7 units, i.e. from 7.0 to 7.7. Such a pH change would substantially alter the solubility and hence plant-availability of nutrients and toxicants (Kirk, 2004). For example, a pH increase in this range would make soil organic ligands more soluble, and thereby solubilise soil Zn (Affholder et al., 2016). In ‘iron toxic’ rice soils, where large concentrations of dissolved ferrous iron can severely damage the plants (Becker & Asch, 2005), H^+ consumption in CO_2 venting could moderate the acidification of the rhizosphere caused by ferrous iron oxidation ($4\text{Fe}^{2+} + \text{O}_2 + 10\text{H}_2\text{O} = 4\text{Fe}(\text{OH})_3 + 8\text{H}^+$) and so limit the impairment of cation uptake caused by acidification (Begg et al., 1994).

The likely importance of carbonic anhydrase (CA) in facilitating CO_2 entry into the root and aerenchyma (Section 4.2) raises a possible link to the plant Zn nutrition. The active centre in all known plant CAs contains Zn (DiMario et al., 2017), and Zn-deficient plants can have impaired CA activity (Sasaki, Hirose, Watanabe & Ohsughi, 1998). Consistent with

this, Affholder et al. (2017) found less CO₂ venting through a rice genotype sensitive to soil Zn deficiency compared with a tolerant genotype.

What factors could be manipulated by plant breeding or crop management to influence soil CO₂ uptake by rice roots? The extent of aerenchyma development and gas barriers in the root wall will be important, both for CO₂ transmission and for oxidation of CH₄ to CO₂ in the rhizosphere; there are differences in both of these between rice genotypes (Yamauchi et al., 2018). There are also genotype differences in CA expression in rice (Xu, Zhang, Guan, Takano & Liu, 2007).

5 | CONCLUSIONS

1. Venting through the roots of CO₂ formed in root and soil respiration is an important control on root and soil CO₂ concentrations in submerged wetland soils over a wide range of plant and soil conditions.
2. We measured rates of CO₂ uptake by roots equivalent to a third of the daily CO₂ fixation in photosynthesis. Without this venting through the roots, the concentrations of CO₂ and associated HCO₃⁻ in root cells would have been well above levels known to be toxic to roots.
3. The removal of CO₂ and hence H₂CO₃ from the soil was sufficient to increase the rhizosphere pH close to the roots by 0.7 units. That is sufficient to solubilise or immobilise various nutrients and toxicants, and potentially provides an explanation for genotype differences in tolerance of nutrient deficiencies and mineral toxicities.
4. The image-based mathematical modelling method that we used, linked to non-invasive X-ray CT imaging, is a powerful way of studying below-ground plant-soil interactions.

REFERENCES

- Affholder, M.C., Weiss, D.J., Wissuwa, M., Johnson-Beebout, S. & Kirk, G.J.D. (2017). Soil CO₂ venting as one of the mechanisms for tolerance of Zn deficiency by rice in flooded soils. *Plant, Cell & Environment*, 40, 3018–3030.
- Arah, J.R.M. & Kirk, G.J.D. (2000). Modelling rice plant-mediated methane emission. *Nutrient Cycling in Agro-Ecosystems*, 58, 221–230.
- Balkos, K.D., Britto, D.T. & Kronzucker, H.J. (2010). Optimization of ammonium acquisition and metabolism by potassium in rice (*Oryza sativa* L. cv. IR-72). *Plant, Cell & Environment*, 33, 23–34.
- Becker, M. & Asch, F. (2005). Iron toxicity in rice—conditions and management concepts. *Journal of Plant Nutrition & Soil Science*, 168, 558–573.
- Beckett, P.M., Armstrong, W., Justin, S.H.F.W. & Armstrong, J. (1988). On the relative importance of convective and diffusive gas flows in plant aeration. *New Phytologist*, 110, 463–468.
- Begg, C.B.M., Kirk, G.J.D., MacKenzie, A.F. & Neue, H.-U. (1994). Root-induced iron oxidation and pH changes in the lowland rice rhizosphere. *New Phytologist*, 128, 469–477.
- Bloemen, J., McGuire, M.A., Aubrey, D.A., Teskey, R.O. & Steppe, K. (2013). Transport of root-respired CO₂ via the transpiration stream affects above-ground carbon assimilation and CO₂ efflux in trees. *New Phytologist*, 197, 555–565.
- Britto, D.T. & Kronzucker, H.J. (2005). Nitrogen acquisition, PEP carboxylase, and cellular pH homeostasis: new views on old paradigms. *Plant, Cell & Environment*, 38, 1396–1409.
- Brix, H. (1990). Uptake and photosynthetic utilization of sediment-derived carbon by *Phragmites australis* (Cav.) Trin. ex Steudel. *Aquatic Botany*, 38, 377–389.

- Butterbach-Bahl, K., Papen, H. & Rennenberg, H. (1997). Impact of gas transport through rice cultivars on methane emission from rice paddy fields. *Plant, Cell & Environment*, 20, 1175–1183.
- Cho, R., Schroth, M.H. & Zeyer, J. (2012). Circadian methane oxidation in the root zone of rice plants. *Biogeochemistry*, 111, 317–330.
- Constable, J.V.H. & Longstreth, D.J. (1994). Aerenchyma carbon dioxide can be assimilated in *Typha latifolia* L. leaves. *Plant Physiology*, 106, 1065–1072.
- DiMario, R.J., Clayton, H., Mukherjee, A., Ludwig, M. & Moroney, J.V. (2017). Plant carbonic anhydrases: Structures, locations, evolution, and physiological roles. *Molecular Plant*, 10, 30–46.
- Fairhurst, T.H., Witt, C., Buresh, R.J. & Dobermann, A. (eds). (2007). *Rice: A Practical Guide to Nutrient Management* (2nd ed.). Manila: International Rice Research Institute.
- Felle, H.H. (2001). pH: Signal and messenger in plant cells. *Plant Biology*, 3, 577–591.
- Geilfus, C.-M. (2017). The pH of the apoplast: dynamic factor with functional impact under stress, *Molecular Plant*, 10, 1371–1386.
- Greenland, D.J. (1997). *The Sustainability of Rice Farming*. Wallingford: CAB International.
- Greenway, H., Armstrong, W. & Colmer, T.D. (2006). Conditions leading to high CO₂ (>5 kPa) in waterlogged–flooded soils and possible effects on root growth and metabolism. *Annals of Botany*, 98, 9–32.
- Hernández, M., Dumont, M.G., Yuan, Q. & Conrad, R. (2015). Different bacterial populations associated with the roots and rhizosphere of rice incorporate plant-derived carbon. *Applied Environmental Microbiology*, 81, 2244–2253.
- Higuchi, T., Yoda, K. & Tensho, K. (1984). Further evidence for gaseous CO₂ transport in relation to root uptake of CO₂ in rice plant. *Soil Science & Plant Nutrition*, 30, 125–136.

Izquierdo, M., Impa, S.M., Johnson-Beebout, S.E., Weiss, D.J. & Kirk, G.J.D. (2016).

Measuring isotopically-exchangeable Zn in submerged Zn-deficient rice soils. *European Journal of Soil Science*, 67, 51–59.

Jiang, Y., van Groenigen, K.J., Huang, S., Hungate, B.A., van Kessel, C., Hu, S., Zhang, J., Wu, L., Yan, X., Wang, L., Chen, J., Hang, X., Zhang, Y., Horwath, W.R., Ye, R.,

Linquist, B.A., Song, Z., Zheng, C., Deng, A. & Zhang, W. (2017). Higher yields and lower methane emissions with new rice cultivars. *Global Change Biology*, 23, 4728–4738.

Keyes, S., Daly, K.R., Gostling, N.J., Jones, D.L., Talboys, P., Pinzer, B.R., Boardman, R., Sinclair, I., Marchant, A. & Roose, T. (2013). High resolution synchrotron imaging of wheat root hairs growing in soil and image based modelling of phosphate uptake. *New Phytologist*, 198, 1023–1029.

Kirk, G.J.D. (2003). Rice root properties for internal aeration and efficient nutrient acquisition. *New Phytologist*, 159, 185–194.

Kirk, G.J.D. (2004). *The Biogeochemistry of Submerged Soils*. Chichester: Wiley.

Kirk, G.J.D. & Bajita, J.B. (1995). Root-induced iron oxidation, pH changes and zinc solubilization in the rhizosphere of lowland rice. *New Phytologist*, 131, 129–137.

Kirk, G.J.D. & Kronzucker, H.J. (2005). The potential for nitrification and nitrate uptake in the rhizosphere of wetland plants: a modelling study. *Annals of Botany*, 96, 639–646.

Kirk, G.J.D., Solivas, J.L. & Alberda, M.A. (2003). Effects of redox conditions on solute diffusion in soil. *European Journal of Soil Science*, 54, 617–624.

Kronzucker, H.J., Siddiqi, M.Y., Glass, A.D.M. & Kirk, G.J.D. (1999). Nitrate-ammonium synergism in rice: a subcellular flux analysis. *Plant Physiology*, 119, 1041–1045.

Maurer, D., Kiese, R., Kreuzwieser, J. & Rennenberg, H. (2018). Processes that determine the interplay of root exudation, methane emission and yield in rice agriculture. *Plant Biology*, 20, 951–955.

- Mori, A., Kirk, G.J.D., Lee, J.S., Morete, M.J., Nanda, A.K., Johnson-Beebout, S.E. & Wissuwa, M. (2016). Rice genotype differences in tolerance of zinc-deficient soils: evidence for the importance of root-induced changes in the rhizosphere. *Frontiers in Plant Science*, 6, 1160. doi: 10.3389/fpls.2015.01160.
- Nouchi, I., Mariko, S. & Aoki, K. (1990). Mechanisms of methane transport from the rhizosphere to the atmosphere through rice plants. *Plant Physiology*, 94, 59–66.
- Pedersen, O., Pulido, C., Rich, S.M. & Colmer, T.D. (2011). *In situ* O₂ dynamics in submerged *Isoetes australis*: varied leaf gas permeability influences underwater photosynthesis and internal O₂. *Journal of Experimental Botany*, 13, 4691–4700.
- Ponnamperuma, F.N. (1972). The chemistry of submerged soils. *Advances in Agronomy*, 24, 29–96.
- Poschenrieder, C., Fernández, J.A., Rubio, L., Pérez, L., Terés, J. & Barceló, J. (2018). Transport and use of bicarbonate in plants: current knowledge and challenges ahead. *International Journal of Molecular Sciences*, 19, 1352. doi:10.3390/ijms19051352.
- Reid, M.C., Pal, D.S. & Jaffe, P.R. (2015). Dissolved gas dynamics in wetland soils: Root-mediated gas transfer kinetics determined via push-pull tracer tests. *Water Resources Research*, 51, 7343–7357.
- Rose, T.J., Impa S.M., Rose M.T., Pariasca-Tanaka J., Mori A., Heuer S., Johnson-Beebout S.E. & Wissuwa M. (2013). Enhancing phosphorus and zinc acquisition efficiency in rice: a critical review of root traits and their potential utility in rice breeding. *Annals of Botany*, 112, 331–345.
- Sasaki, H., Hirose, T., Watanabe, Y. & Ohsughi, Y. (1998). Carbonic anhydrase activity and CO₂-transfer resistance in Zn-deficient rice leaves. *Plant Physiology*, 118, 929–934.
- Savchenko, G., Wiese, C., Neimanis, S., Hedrich, R. & Heber, U. (2000). pH regulation in apoplastic and cytoplasmic cell compartments of leaves. *Planta*, 211, 246–255.

- Schindelin, J., Arganda-Carreras, I., Frise, E., Kaynig, V., Longair, M., Pietzsch, T., Preibisch, S., Rueden, C., Saalfeld, S., Schmid, B., Tinevez, J.Y., White, D.J., Hartenstein, V., Eliceiri, K., Tomancak, P. & Cardona, A. (2012). Fiji: an open-source platform for biological-image analysis. *Nature Methods*, 9, 676–682.
- Schütz, H., Seiler, W. & Conrad, R. (1989). Processes involved in formation and emission of methane in rice paddies. *Biogeochemistry*, 7, 33–53.
- Shimono, H., Kondo, M. & Evans, J.R. (2019). Internal transport of CO₂ from the root zone to plant shoot is pH dependent. *Physiologia Plantarum*, 165, 451–463.
- Singer, A., Eshel, A., Agami, M. & Beer, S. (1994). The contribution of aerenchymal CO₂ to the photosynthesis of emergent and submerged culms of *Scirpus lacustris* and *Cyperus papyrus*. *Aquatic Botany*, 49, 107–116.
- Takano, J., Noguchi, K., Yasumori, M., Kobayashi, M., Gajdos, Z., Miwa, K., Hayashi, H., Yoneyama, T. & Fujiwara, T. (2002). Arabidopsis boron transporter for xylem loading. *Nature*, 420, 337–340.
- van Bodegom, P., Stams, F., Mollema, L., Boeje, S. & Leffelaar, P. (2001). Methane oxidation and the competition for oxygen in the rice rhizosphere. *Applied Environmental Microbiology*, 67, 3586–3597.
- van der Gon, H.A.C.D., Kropff, M.J., van Breemen, N., Wassmann, R., Lantin, R.S., Aduna, E., Corton, T.M. & van Laar, H.H. (2002). Optimizing grain yields reduces CH₄ emissions from rice paddy fields. *Proceedings of the National Academy of Sciences of the USA*, 99, 12021–12024.
- Wang, J., Akiyama, H., Yagi, K. & Yan, X. (2018). Controlling variables and emission factors of methane from global rice fields. *Atmospheric Chemistry & Physics*, 18, 10419–10431.

- Xu, S., Zhang, X., Guan, Q., Takano, T., & Liu, S. (2007). Expression of a carbonic anhydrase gene is induced by environmental stresses in rice (*Oryza sativa* L.). *Biotechnology Letters*, 28, 89–94.
- Yao, H. & Conrad, R. (2000). Electron balance during steady-state production of CH₄ and CO₂ in anoxic rice soil. *European Journal of Soil Science*, 51, 369–378.
- Yamauchi, T., Colmer, T.D., Pederson, O. & Nakazono, M. (2018). Regulation of root traits for internal aeration and tolerance of waterlogging-flooding stress. *Plant Physiology*, 176, 118–1130.
- Yoshida, S., Forno, D.A., Cook, J.H. & Gomez, K.A. (1976). *Laboratory Manual for Physiological Studies of Rice* (3rd ed.). Manila: International Rice Research Institute.

SUPPORTING INFORMATION

Additional Supporting Information is provided.

TABLE 1 Standard parameter values

Symbol	Definition	Standard value	Comments
L	Soil depth	1.7 dm	Set by experimental conditions
θ	Soil porosity	0.69	Measured
f_L	Soil liquid diffusion impedance factor	0.35	Based on Kirk, Solivas, & Alberto (2003) for similar soils
v	Water flux into roots	0 dm s ⁻¹	At $v = 10^{-7}$ dm s ⁻¹ , which is a typical value (Kirk, 2004), the additional CO ₂ flux into the roots ($= vC_L$) is < 2 % greater. We therefore use $v = 0$ for simplicity
pH	Soil pH	7.0	Measured
$[\text{H}_2\text{CO}_3^*]_0 + [\text{HCO}_3^-]_0$	$\text{H}_2\text{CO}_3^* + \text{HCO}_3^-$ concentration at $z = 0$	1 mM	Measured
$[\text{H}_2\text{CO}_3^*]_i + [\text{HCO}_3^-]_i$	$\text{H}_2\text{CO}_3^* + \text{HCO}_3^-$ concentration in bulk soil at $t = 0$	40 mM	Measured
$[\text{CH}_4]_0$	Dissolved CH ₄ concentration at $z = 0$	2.9 nM	From atmospheric P_{CH_4}
$[\text{N}_2]_0$	Dissolved N ₂ concentration at $z = 0$	0.5 mM	From atmospheric P_{N_2}
$S_{\text{CO}_2,0}$	CO ₂ production from soil C	9.5×10^{-8} mol dm ⁻³ s ⁻¹	Fitted for unplanted soil, such that C_L in the absence of roots (i.e. $k_V = 0$, $k_T = 0$) agrees with measured value
α_{CH_4}	$S_{\text{CH}_4}/S_{\text{CO}_2}$	1.0	Set such that $P_{\text{CH}_4} \approx P_{\text{CO}_2}$
K_θ	Equation 2	2.3×10^{-3}	Fitted for unplanted soil
k_E	Rate constant for ebullition	1.0×10^{-4} s ⁻¹	Fitted
k_T	Root gas transmissivity	9.5×10^{-4}	Fitted
k_V	Constant for decomposition of root-derived C	9.3×10^{-13} mol dm ⁻¹ s ⁻¹	Fitted

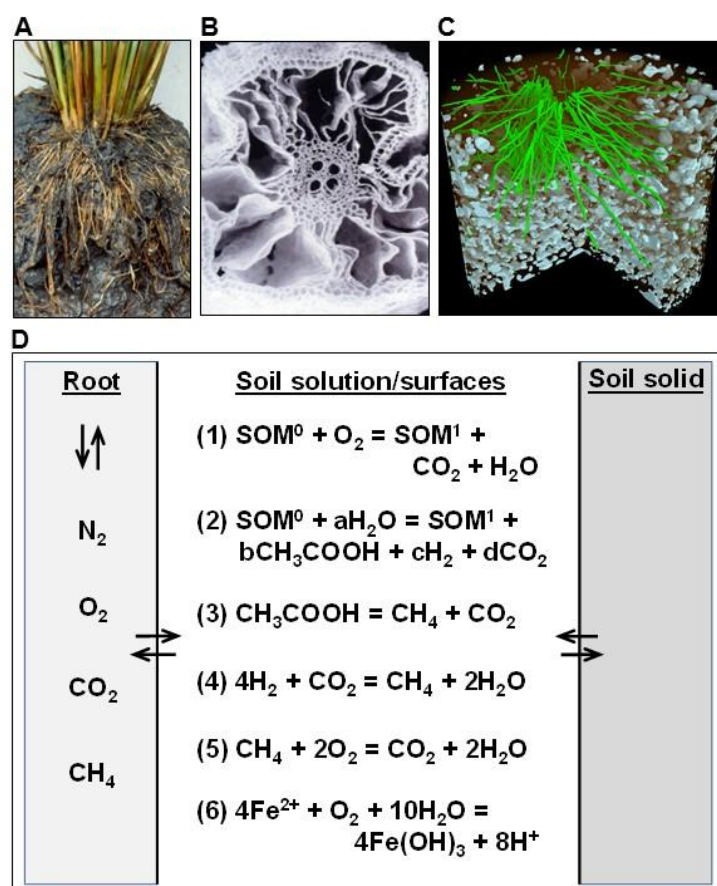


FIGURE 1 Gas formation and venting through rice roots in paddy soil. (A) Cross-section showing roots and water-saturated, anaerobic soil. (B) Root aerenchyma. (C) Cut-away X-ray CT image of roots (green) and soil gas bubbles (white). (D) Gas generating and consuming processes in the soil (after inorganic oxidants have been exhausted): (1) aerobic decomposition of soil organic matter (SOM) in the rhizosphere, (2) anaerobic decomposition of SOM in the soil bulk (a-d are coefficients), (3) CH_4 production from acetate, (4) CH_4 production from H_2 , (5) CH_4 oxidation, (6) Fe(II) oxidation. Gas bubbles become entrapped under soil particles, but there is no continuous gas phase through the soil.

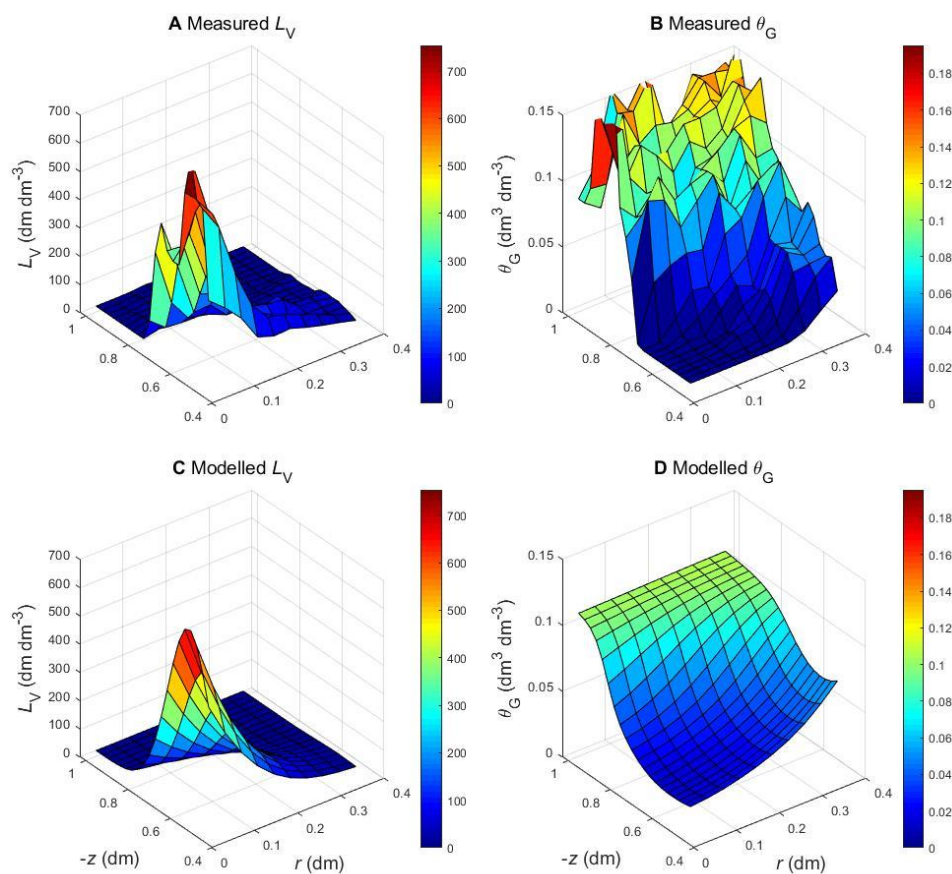


FIGURE 2 Measured and modelled results. (A), (C) Root length density (L_V) and (B), (D) volumetric soil gas content (θ_G). The measured data are for a single replicate with 4 plants per pot. The modelled L_V data are fits to a bimodal Gaussian distribution (Equation 7); the modelled θ_G data are fits of the gas formation and transport model (Equations 1–6). Depth, z , is depth below floodwater-soil boundary; radius, r , is radial distance from the vertical axis through the middle of the plants.

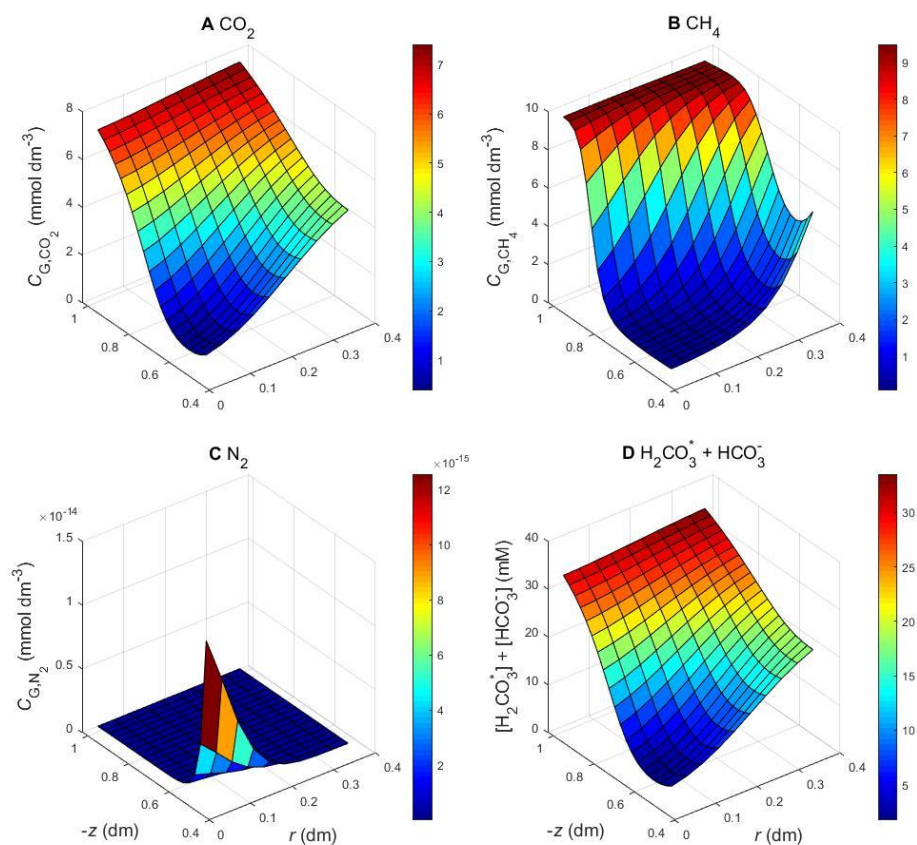


FIGURE 3 Modelled distributions of gases in the soil. (A)–(C) Concentrations of CO_2 , CH_4 and N_2 gases in soil air. (D) Concentrations of dissolved CO_2 ($[\text{H}_2\text{CO}_3^*] = [\text{CO}_2] + [\text{H}_2\text{CO}_3]$) + HCO_3^- ($[\text{HCO}_3^-] = K_1[\text{H}_2\text{CO}_3^*]/[\text{H}^+]$ where K_1 = apparent 1st dissociation constant of H_2CO_3) in soil solution. Parameter values and root distribution as in Figure 2.

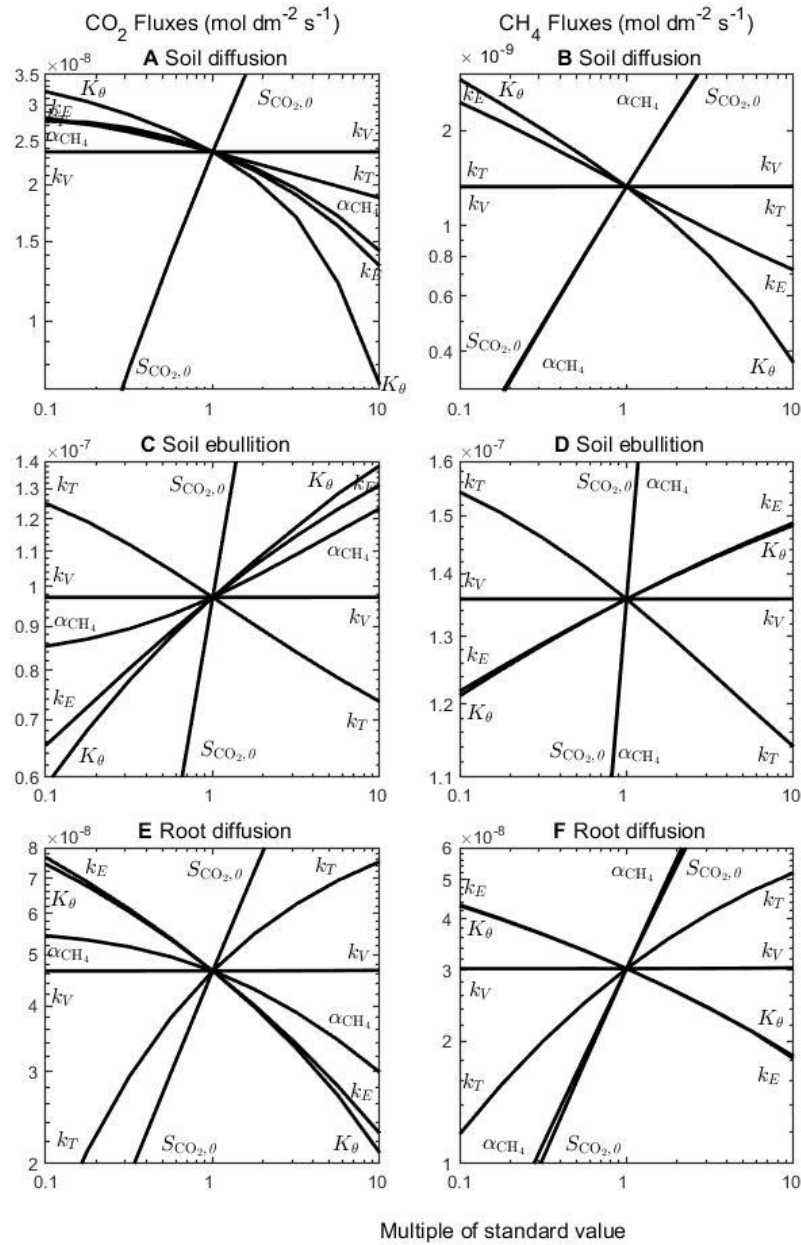


FIGURE 4 Sensitivity of model to root gas transmissivity (k_T), ebullition rate constant (k_E), constant for decomposition of root-derived carbon (k_V), initial soil CO₂ production ($S_{\text{CO}_2,0}$), ratio of CH₄ to CO₂ production (α_{CH_4}) and K_θ in Equation 2. Other parameters as for Figures 2 and 3 (Table 1).